

# Using CFD Capabilities of CONTAM 3.0 for Simulating Airflow and Contaminant Transport in and around Buildings

**Liangzhu (Leon) Wang, PhD**  
Associate Member ASHRAE

**W. Stuart Dols**  
Member ASHRAE

**Qingyan Chen, PhD**  
Fellow ASHRAE

*Received March 20, 2010; accepted August 9, 2010*

---

*CONTAM is a multizone building airflow and contaminant transport computer program often used for ventilation and indoor air quality analysis. The program was recently enhanced to incorporate CFD capabilities for both outdoor and indoor environmental analysis. This paper introduces the CFD features implemented within the most recent version, CONTAM 3.0. The outdoor or external CFD link predicts wind pressure coefficients and contaminant concentrations for airflow paths at the building surface. A converter computer program translates the wind pressure coefficients to the CONTAM data format. This external CFD link is useful for parametric studies of the impact of outdoor air quality on indoor environment when considering different wind directions or contaminant locations, especially simulations under transient conditions. The ability to embed a single CFD zone in a CONTAM network model has also been implemented. This enables the detailed modeling of a zone when the well-mixed multizone assumption is not appropriate and then uses the multizone approach for the rest of a building, thus capturing the local distribution of air and contaminant properties in a zone and their impacts on other zones of a building. CFD capabilities are demonstrated using a generic residential house model to show how these two new CFD features enhance the existing CONTAM capabilities for both indoor and outdoor air quality analysis.*

---

## INTRODUCTION

Building ventilation design and indoor air quality (IAQ) analysis involve evaluations of both bulk and detailed air properties in buildings. One of the most commonly used building ventilation tools for bulk airflow analysis is multizone network modeling. In a multizone building model, airflow and species transport are calculated between the rooms of a building and between the building and the outdoors. The so-called well-mixed assumption, in which each zone is characterized by a single contaminant concentration, is used to make the bulk analysis simpler and faster. Under the well-mixed assumption, a building is subdivided into zones having homogeneous air properties and species concentrations. When air and species properties are highly non-uniform, the well-mixed assumption is not valid. For these situations, a tool to calculate detailed air properties, such as computational fluid dynamics (CFD), is needed. Compared to a multizone model, CFD is more computationally intensive and is less often used for whole-building analysis or longer-term transient simulations. Table 1 lists some of the pros and cons of multizone and CFD models. The multizone model is faster with broader assumptions,

---

**Liangzhu Wang** is an assistant professor in the Department of Building, Civil and Environmental Engineering at Concordia University, Montreal, Quebec. **W. Stuart Dols** is a mechanical engineer with the Indoor Air Quality and Ventilation Group of the Building and Fire Research Laboratory at the National Institute of Standards and Technology, Gaithersburg, MD. **Qingyan Chen** is a professor in the School of Mechanical Engineering at Purdue University, West Lafayette, IN.

**Table 1. Comparison of Multizone and CFD Models**

	<b>Multizone</b>	<b>CFD</b>
<b>Simulation assumptions</b>		
Uniform contaminant concentration in each room	Yes	No
Quiescent or still air in each room	Yes	No
Neglect air resistance in each room	Yes	No
Neglect inflow momentum effect, if any	Yes	No
Instantaneous contaminant transport inside room	Yes	No
Hydrostatic distribution of pressure inside room	Yes	No
<b>Simulation capabilities</b>		
Whole-building and yearly dynamic simulations	Better	
Modeling building air infiltration	Better	
Computational speed	Better	
Modeling spatial airflow and contaminant concentration		Better
Modeling wind pressure on buildings		Better
Modeling large openings and spaces		Better
Modeling spatial personal exposure		Better

whereas the CFD is more accurate (if used correctly) but with more computational cost. The multizone model provides average characteristics of airflow and contaminant transport phenomena, while the CFD method can predict spatial distributions of these parameters. For building ventilation design and IAQ analysis, the multizone and CFD models are not conflicting methods but can be used as appropriate to take advantage of the benefits offered by each. However, up until recently, the analyst had to choose between using one or the other modeling approach.

The idea of coupling multizone and CFD models was proposed by Schaelin et al. (1993), via the method of detailed flow path values. This method was meant to improve upon the well-mixed assumption by using CFD to calculate pressures, velocities, and contaminant concentrations near flow paths and then using them as inputs to multizone simulations. They demonstrated the method through manual exchange of boundary conditions between two stand-alone programs and showed promising results. Soon thereafter, Clarke et al. (1995) and Negrao (1998) started to implement an automatically coupled CFD and network model inside the Environmental Systems Performance, Research version (ESP-r) building simulation program (Clarke 1985). Bartak et al. (2002) then adopted a conflation controller (Beausoleil-Morrison 2002) to improve the coupled module of ESP-r. Their work provided one of the earliest coupled CFD and network models. Some applications of coupled CFD and multizone methods and some experimental studies were conducted by Srinivas (2001), Jayaraman et al. (2004), and Srebric et al. (2008). Their studies showed that coupling a CFD model with a multizone model could obtain more realistic predictions of airflow and contaminant transport in buildings with large spaces. However, these studies were mostly research-oriented and did not provide a general, more widely available design tool. Some commercial software is available with integrated building energy

simulation and CFD capability, but none specifically developed for building ventilation and IAQ analyses.

Aiming at developing a public-domain tool for building ventilation design and indoor air quality analyses for the general public, this study has coupled CONTAM (Walton and Dols 2008), a multizone network software program developed at the National Institute of Standards and Technology (NIST), with CFD0, a CFD software tool with an indoor zero-turbulence model (Chen and Xu 1998). CONTAM is a popular tool to determine building air infiltration, exfiltration, and room-to-room airflows driven by wind pressures on building exteriors, buoyancy effects related to the indoor and outdoor air temperature difference, and mechanical ventilation. It also predicts the dispersal of airborne contaminants and can be used to calculate personal exposure to contaminants. CONTAM includes a Microsoft Windows<sup>®</sup>-based front end, ContamW, and a console solver program, ContamX. The first version of ContamW was released in 1996, whereas ContamX evolved from AIRNET (Walton 1989). CFD0 was a CFD program originally developed for ASHRAE research project RP-927 (Chen et al. 1999), and improved by Wang (2007). Wang and Chen (2007a, 2007b) studied the solution characteristics of integrated multizone and CFD models, developed the coupling algorithm, and validated the coupled CONTAM and CFD0 program. In this paper, the coupling algorithm is implemented in a new version of CONTAM to be released as CONTAM 3.0. This paper first introduces the algorithm for two methods of linking CONTAM and CFD0, the external link for performing external airflow analysis, and the internal link for embedding a CFD0 zone in a CONTAM airflow and contaminant transport network. A demonstration case of a generic single-family house is presented for the analysis of wind pressures on the building enclosure and indoor air quality.

## METHODS OF CONTAM AND CFD0 INTEGRATION

Incorporation of CFD0 into CONTAM 3.0 provides two major capabilities: linking information on exterior wind pressures and outdoor contaminant concentrations to CONTAM's indoor simulations, and embedding detailed CFD zones in the CONTAM airflow and contaminant transport network.

### Linking of CFD and CONTAM for Building Exterior Simulations

Wind pressure is a major driving force for air infiltration through the building envelope. Wind pressure, as a function of wind speed, wind direction, building configuration, and local terrain effects (ASHRAE 2009), can be accounted for by CONTAM with one of three options: specifying wind pressure to be constant, implementing surface averaged wind pressure profiles for each envelope penetration, and using spatially and time-varying wind pressures based on an external wind pressure and contaminant (WPC) file. A general approach for handling the variable effects of wind is to use a local wind pressure coefficient  $C_p$ , which is a function of air density  $\rho$ , local wind pressure,  $P_w$ , undisturbed wind speed  $U_H$ , and wind pressure  $P_H$ , at a reference height  $H$  in the far airflow field.

A rough estimate of the average wind pressure profile over each side of a building surface can be obtained from empirical or experimental studies, such as Swami and Chandra (1988), as a function of wind direction relative to a building surface (i.e., relative wind direction). In fact, air movement around buildings is a three-dimensional turbulent flow, so wind pressures could vary significantly even over a single building surface. Therefore, surface-averaged wind pressure coefficients may be insufficient for air infiltration predictions (Gao 2002). A more accurate approach is to address the variations of wind pressure coefficients at each location over a building surface. The most reliable means of determining  $C_p$  for a specific building are through on-site measurements or wind tunnel studies (Persily and Ivy 2001). However, these measurements can be expensive and technically difficult. CFD simulations of turbulent flows around

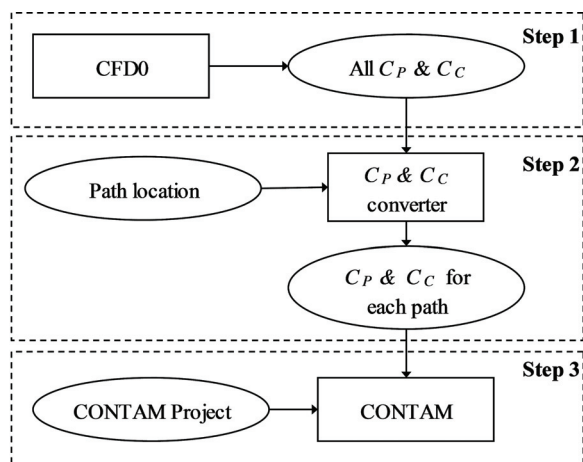


**Figure 1. Schematic of link between CONTAM and CFD0 for building external airflow and contaminant transport simulations.**

buildings can be an alternative to obtain wind pressures, as demonstrated by Gao (2002) and Jiang (2003). More importantly, using CFD for simulating external contaminant releases can provide detailed profiles of contaminant concentration on building exteriors, which are useful to study the impact of outdoor air quality on an indoor environment (Wang and Emmerich 2010).

The prior version of CONTAM, 2.4c, provides the capability of implementing spatially and time-varying wind pressures and outdoor contaminant concentrations using the external WPC file. However, a WPC file is created by a CFD analysis for a specific wind speed and direction. In comparison, the external CFD link in CONTAM 3.0 calculates a profile of wind pressure coefficients for each building leakage path and for a range of wind directions. This approach avoids the need for an additional CFD run whenever the wind direction or speed changes. The external CFD0 link is comprised of three steps, as shown in Figure 1. First, CFD0 calculates airflow and contaminant transport outside a building and creates a file with all wind pressure coefficients ( $C_p$ ) or contaminant concentrations ( $C_c$ ) over the building surfaces. A separate computer program then searches in the files for the values of  $C_p$  or  $C_c$  for each envelope airflow path for which a location is defined in the CONTAM project. The program then converts the values to a CONTAM library file with  $C_p$  or  $C_c$  values for all envelope airflow paths. Finally, when a CONTAM simulation is performed using a CONTAM weather file, the appropriate  $C_p$  or  $C_c$  for each envelope airflow path is utilized for each wind direction and simulation time step.

The three-step procedure in Figure 1 provides a flexible external link between CONTAM and CFD0 that can be used for the following types of studies:

- **Wind pressure and/or outdoor contaminant concentrations that vary with wind direction.** In the first step, different wind directions can be defined, for example, from  $0^\circ$  to  $360^\circ$  around the building. CFD0 calculates and automatically saves envelope  $C_p$  or  $C_c$  for all wind directions. When a CONTAM simulation needs to consider different wind direction, it uses the saved  $C_p$  or  $C_c$  values without having to run the CFD simulation again.
- **Variable locations of outdoor contaminant sources.** In the first step, CFD0 saves all calculated air properties and velocities, which can be reused if the locations of outdoor contaminant

sources change, assuming this change does not affect the airflow field. This feature is useful for parametric study of contaminant source locations on indoor concentration levels.

- **Transient contaminant transport outdoors using previously calculated external airflows at steady state.** Similar to the above feature, this option allows users to run a transient outdoor contaminant transport simulation using steady-state outdoor airflow results already available without the need to rerun the external CFD airflow calculations.

The external CFD link in CONTAM 3.0 has been applied to the study of indoor exposure to carbon monoxide caused by operating gasoline-powered electric generators outside of an existing manufactured house and a hypothetical two-story house (Wang and Emmerich 2010; Wang et al. 2010). This study involved an examination of many parameters, including contaminant source location and weather conditions, and the external CFD link reduced the computational cost significantly.

### **Embedding CFD Zone within a CONTAM Airflow Network**

The well-mixed assumption of multizone models is less suitable for zones with nonuniform distribution of air properties and contaminant concentrations (Wang and Chen 2008). An example is a large atrium in a multistory building. One approach to this situation is for the large space to be handled by CFD0 and the rest of the zones in the building by CONTAM, with the two programs exchanging information at the boundaries formed by the airflow paths connecting the CFD and CONTAM zones. Exchanged information at the interfaces include airflow rate, air pressure, and contaminant concentration. To satisfy conservation equations on both sides of the boundaries, the process is often a two-way iterative procedure. This is different from the external link, where the values of  $C_P$  or  $C_C$  are passed one-way from CFD0 to CONTAM. Thus, embedding the CFD zone within CONTAM is also called dynamic coupling of the two methods.

Because dynamic coupling of CONTAM and CFD0 integrates two separate programs, some criteria need to be met to ensure a successful integration. Wang and Chen (2007a) studied the solution characteristics of dynamic coupling and suggested two necessary conditions for a successfully coupled airflow calculations:

- Mass airflow rate predicted by a multizone airflow network model must equal the integral of the mass airflow rate of all CFD grid cells for each interface airflow path to ensure overall mass balance
- The resistance characteristic (i.e., the airflow rate as a function of pressure drop) must be known for each multizone/CFD boundary grid cell to ensure closure of the problem

Given that the boundary conditions are exchanged iteratively between CONTAM and CFD0, the dynamic coupling procedure can be unstable if the boundary conditions are exchanged incorrectly (Negrao 1998; Bartak et al. 2002). Wang and Chen (2007a) suggested that the exchange of pressure boundary conditions between the two programs can achieve an unconditionally stable solution, whereas other types of information exchange, such as mass flow rates, may lead to divergence. Moreover, to link two separate programs with distinct program modules and data structures, an appropriate programmatic coupling scheme is required. Figure 2 shows the two-step schematic for coupling CONTAM and CFD0 programs in CONTAM 3.0 for a simulation at steady state: coupled airflow simulation and, if necessary, coupled contaminant transport simulation. If an airflow result is available from a previous coupled calculation, it can be imported directly to save extra computational cost. Otherwise, the coupled program performs a fully coupled procedure for airflow prediction. The fully coupled procedure obtains initial values of air pressures and flow rates for all zones by running a CONTAM simulation

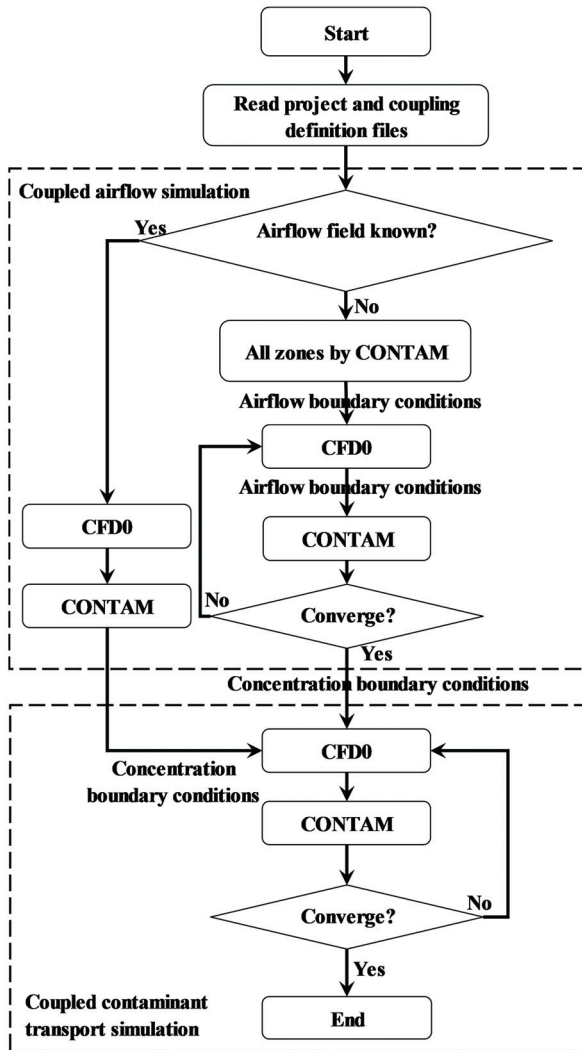


**Figure 2. Schematic of embedding a CFD zone in the CONTAM airflow network for simulations at steady state in CONTAM 3.0.**

for the whole building. With boundary conditions from CONTAM, CFD0 calculates the airflow in the CFD zone and feeds boundary conditions back to CONTAM. The iteration continues until convergence is achieved for both sets of calculations. If a coupled simulation of contaminant transport is needed, a similar iterative procedure is used except that the contaminant concentration is exchanged at each interface airflow path as opposed to the pressures and airflow rates. For a coupled transient simulation, the procedure in Figure 2 is repeated for each time step.

The graphical user interface (GUI) of CONTAM was modified to provide inputs for the CFD-related features. This includes the ability to define coupling methods, coupling convergence factors and iteration limits, and output options for CFD-related results. A separate GUI program

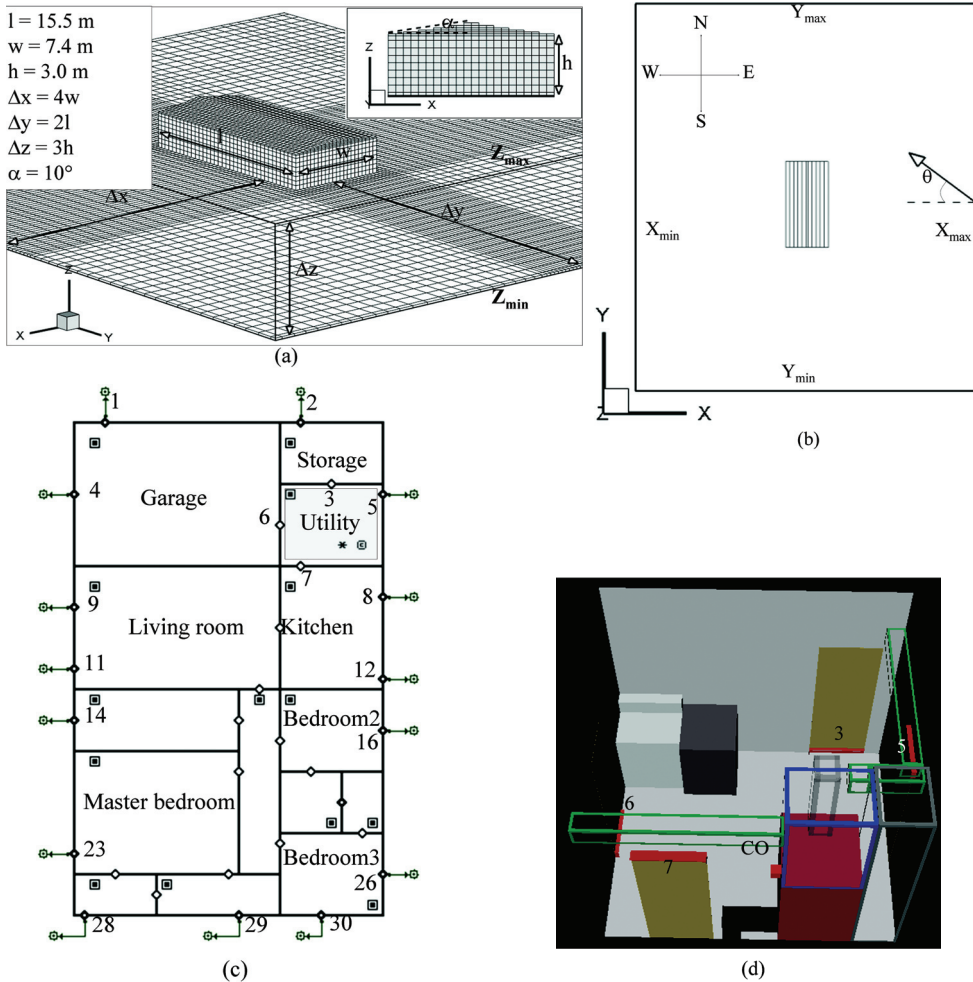


**Figure 3. (a) CFD mesh, (b) plan view of building in CFD, (c) CONTAM zone configuration with shaded zone of the utility room, and (d) internal view of utility room in CFD.**

was also developed to allow the user to graphically define the CFD domain and to review the CFD-related results of the coupled simulation. These new GUI features were developed along with a tutorial with an example problem to allow use of the program with minimal training.

### DEMONSTRATION OF THE CFD CAPABILITIES

A low-rise residential house was modeled in order to demonstrate both the external and internal CFD modeling capabilities of CONTAM 3.0. Figure 3 provides CONTAM and CFD perspectives of the model. Holmes (1986, 1994) measured the wind pressure distribution on a low-rise house model for various wind directions in an open-circuit, boundary-layer wind tunnel. For the purposes of this study, the house model in Holmes' experiment was scaled up to  $15.5 \text{ m} \times 7.4 \text{ m} \times 3.0 \text{ m}$  ( $50.9 \text{ ft} \times 24.3 \text{ ft} \times 9.8 \text{ ft}$ ) ( $L \times W \times H$ ) (the height excluding the sloped roof), as illustrated in Figure 3a. The external CFD link with CONTAM is demonstrated by using CFD0 to calculate wind pressure profiles for each airflow path of the house envelope.

Figure 3b shows the plan view of the house in CFD0. Infiltration rates were then calculated using CONTAM with the zone configuration presented in Figure 3c. The internal CFD link is demonstrated by simulating the transport of carbon monoxide (CO) in the house produced by a faulty furnace in the utility room, the CFD model for which is shown in Figure 3d.

### Prediction of Wind Pressure Profiles and Infiltration Rates

The external CFD simulation of the house used a total grid number of  $74 \times 87 \times 24$  ( $X \times Y \times Z$ ), as shown in Figure 3a. The wind velocity profile at the domain boundary was selected to represent an "urban and suburban location" (ASHRAE 2009), similar to that in Holmes' experiment. CFD0 simulations of wind were performed for the relative wind direction  $\theta$  between  $0^\circ$  and  $360^\circ$ , with  $30^\circ$  increments. Figure 3b shows that the relative wind direction to a building surface at a specific envelope location is defined as the clockwise angle from the building surface azimuth angle to the wind azimuth angle (Walton and Dols 2008). The simulation for each wind direction took between 300 and 400 iterations to converge, with a convergence criterion of  $1 \times 10^{-3}$ . The total simulation time for all 13 wind directions was about 8 h on a desktop PC with an Intel Pentium 4 2.0 GHz microprocessor. The external CFD0 link calculates a wind pressure coefficient for every relative wind direction at the location of each envelope airflow path.

Figure 4 shows the calculated wind pressure coefficients versus relative wind direction for each path at the surface of the house as compared to the surface-averaged wind pressure coefficient (Swami and Chandra 1987) and the measurements by Holmes (1986, 1994). As seen in these plots, wind pressure profiles show a strong dependence on path locations. They also change dramatically with wind direction, especially for paths near the edge of the building surface. The surface-averaged value of  $C_p$  (dashed lines) does not exhibit this variation with path location. The surface-averaged  $C_p$ s are also symmetric about the relative wind direction of  $180^\circ$ , which, in reality, would only be valid for the envelope locations on the vertical symmetry line of a building façade.

Compared to the measurements by Holmes (1986, 1994), the external CFD0 link generally predicted the wind pressure profiles reasonably well, with some exceptions. The most significant exception was observed for Path 28 for a relative wind direction of  $90^\circ$ , as marked by the dot and arrow in Figure 4 (bottom left). The discrepancy could be caused by the inability of CFD0 to predict wind pressures correctly in the regions with strong turbulence separations and recirculation flows near that path. In fact, the Reynolds Averaged Navier-Stokes (RANS) equations were found incapable of resolving the turbulence vortices and the curvature-sensitive separation flow features in wind flow around buildings (Cochran 2000), and are also not able to capture the time-dependent nonhomogenous and/or anisotropic flows. Using a single turbulence model for each turbulence scale, RANS models focus on time-averaging flow features and their interactions with turbulence effects (time-wise turbulence fluctuations). A better option may be large eddy simulation (LES) models, which solve spatially filtered unsteady Navier-Stokes equations. LES is capable of accounting for the interactions between size-resolved large-scale eddies and unresolved smaller eddies (space-wise turbulence structures), for which turbulence effects are not averaged over time, so an unsteady calculation is performed. RANS models have a lower computational cost than LES models, but they are not as good as LES for capturing time-dependent anisotropic large eddies, which occur in outdoor flows. As a RANS model, CFD0 uses an indoor air zero-equation model for turbulence closure and has limited capabilities for outdoor airflows. Efforts to improve CFD capabilities in CONTAM for such airflows are under development (Wang et al. 2010).

A primary use of the wind pressure profile prediction method presented here is calculating building air infiltration rates. Therefore, it is useful to compare the air infiltration rate calculated using the various methods of obtaining wind pressure coefficients. The measured data

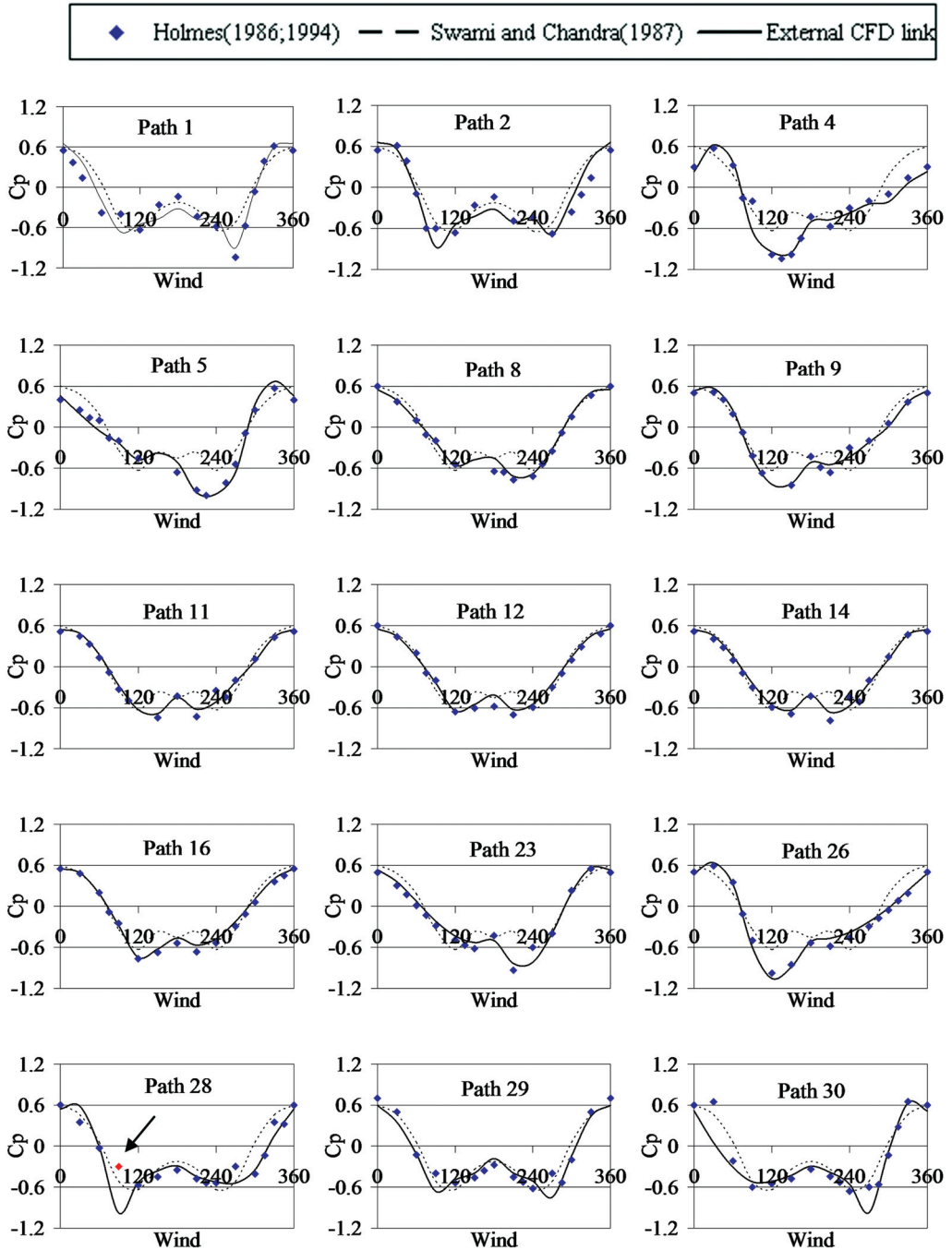


**Figure 4. Comparison of calculated profiles of wind pressure coefficient by the external CFD link, measured data at each airflow path (Holmes 1986, 1994), and average data for each building surface (Swami and Chandra 1987) of the house.**

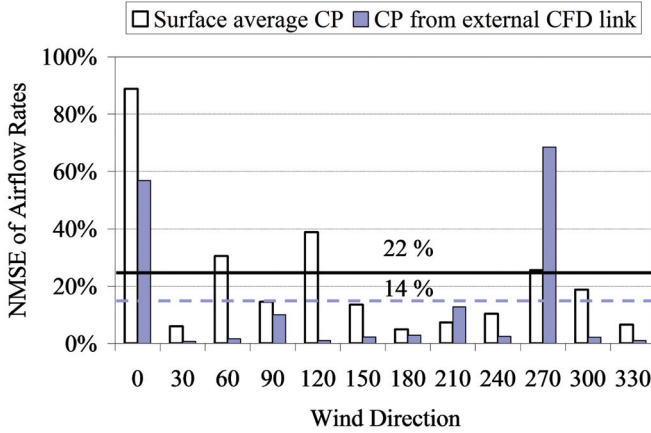


**Figure 5. NMSE of predicted airflow rates under different wind directions using averaged wind pressure coefficients (Swami and Chandra 1987) and predicted values from the external CFD link.**

from Holmes (1986, 1994) were used as a baseline for comparison. Results of the comparison are shown in Figure 5, with the normalized mean square error (NMSE) (ASTM 2008) as defined by Equation 1, which is a measure of the magnitude of difference relative to  $F_a$  and  $F_b$ .

$$NMSE = \frac{1}{(\overline{F_a})(\overline{F_b})} \left[ \frac{1}{n} \sum_{i=1}^n (F_{a,i} - F_{b,i})^2 \right] \quad (1)$$

where

$n$  = total number of envelope airflow paths

$F_{b,i}$  = predicted airflow rate for path  $i$  by baseline method

$\overline{F_a}$  = average absolute value of all envelope airflow rates by baseline method

$\overline{F_b}$  = average absolute value of all envelope airflow rates by alternative method

Figure 5 illustrates that the external CFD link generally predicted airflows better than using the surface-averaged wind pressure profiles: the NMSE was 14% compared to 22% when the surface-averaged  $C_p$ s were used. For wind out of the north ( $0^\circ$  in Figure 5), the NMSE of predicted airflow rates using the surface-averaged  $C_p$  was over 80%, whereas it was 57% using  $C_p$ s from the external CFD link. The worst case for the external CFD link was for the wind direction of  $270^\circ$ , for which comparisons are provided between the predicted airflows of the individual envelope flow paths in Figure 6. Most of the airflows determined using the external link were relatively close to those determined using the measured wind pressure data, except for path 28. When the wind direction was  $270^\circ$ , the relative wind angle for path 28 was  $90^\circ$ . As shown in Figure 4, the predicted  $C_p$  value (highlighted by the dot with arrow) determined using the external CFD link was three times higher than the measured value. These examples show how variation of wind pressures can affect infiltration predictions significantly.

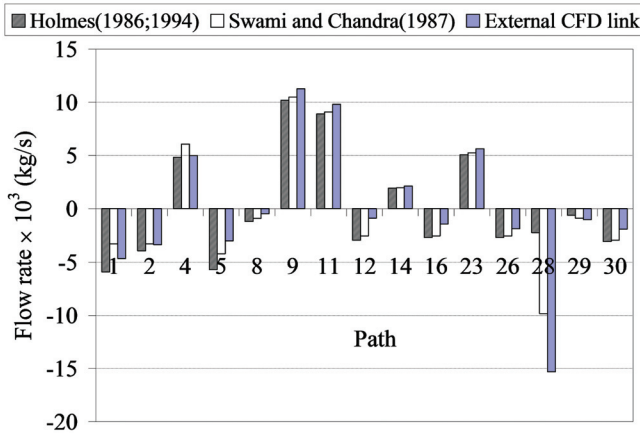


**Figure 6. Comparison of calculated infiltration rates using wind pressure coefficients predicted by the external CFD link, measured data from Holmes (1986, 1994), and surface-averaged data from Swami (1987) when the wind is out of the west (270°).**

**Table 2. Predicted Airflow Rates of Airflow Paths in Utility Room (Negative Value Shows Outflow from Room)**

Airflow Path	Path 3	Path 5	Path 6	Path 7
Airflow Rate × 10 <sup>3</sup> m <sup>3</sup> /s (× 10 <sup>2</sup> ft <sup>3</sup> /s)	5.5 (19.4)	5.6 (19.8)	-0.9 (-3.2)	-10.6 (-37.4)

### Prediction of Indoor Contaminant Transport

The same low-rise residential house was used to demonstrate the embedding of a CFD zone within a CONTAM airflow network. For the purpose of this simulation, it was assumed that the gas furnace in the utility room (the shaded zone in Figure 3c) was malfunctioning and releasing carbon monoxide (CO) into the building. In order to investigate the effects of nonuniformity of CO concentration in the utility room, it was simulated by CFD0, and the remaining rooms were simulated as well-mixed zones.

The following describes the inputs used to establish the test case. The utility room is 3.2 m × 2.6 m × 2.7 m (10.5 ft × 8.5 ft × 8.9 ft) ( $L \times W \times H$ ) with a total CFD grid of 70 × 70 × 90. Ambient air temperature was set to 25°C, and the wind was set to 10 m/s (32.8 ft/s) from 30° relative to the north. CO source strength was set to 126.6 g/h (4.5 ounce/h), which was determined from a CO emission rate of 1 mg/kJ ( $3.7 \times 10^{-5}$  ounce/Btu) by a previous experimental study (Ryan and McCrillis 1994) and a furnace power output of 35.2 kW (120 000 Btu/h) from another study (Lee 1990). The furnace was run under a 10-minute on/off cycle. Figure 3d illustrates the CO source location, furnace, and the four airflow paths that were modeled as cracks located at either the top or bottom of the doors. Airflow was assumed to be steady, and the time-dependent transport of CO was simulated for 2 h with a one-minute time step. Typically, for coupled CO simulations, only two exchanges of boundary conditions were required between the multizone and CFD calculation regimes. The 2 h transient multizone/CFD simulation of CO distribution converged at each time step with a convergence criterion of 0.01 and required a total simulation time of about 13 h on a desktop PC with an Intel 2.66 GHz microprocessor.

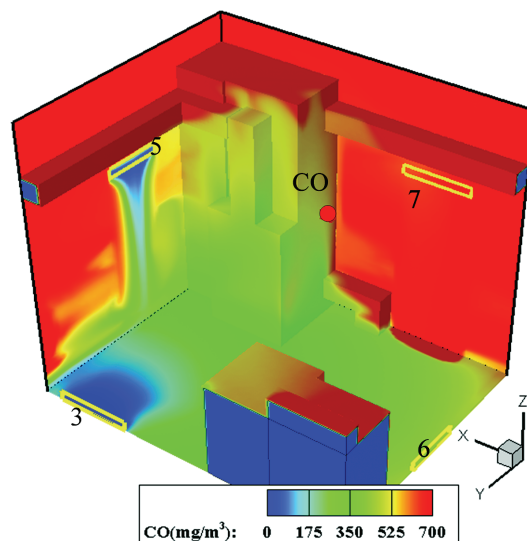


**Figure 7. Distribution of CO concentration ( $\text{mg}/\text{m}^3$ ) in utility room at end of 2 h simulation time ( $1 \text{ mg}/\text{m}^3 \approx 9.9 \times 10^{-7} \text{ oz}/\text{ft}^3$ ).**

Table 2 provides the calculated airflow rates through the door cracks of the utility room. There were two air inflows to the room: from the storage room through path 3 and from the outside through path 5. Most of the outflow goes to the kitchen through path 7, and the rest to the garage through path 6.

With the calculated airflow rates as inputs, CFD0 calculated the time-dependent CO distribution in the utility room over 2 h. Local values of CO concentration were provided near the airflow paths in the utility room for the CONTAM simulation of the rest of the rooms of the house. As shown in Figure 7, at end of the two-hour simulation time the CO levels in the utility room were non-uniform. The CO concentration was close to zero near paths 3 and 5 due to the inflow of uncontaminated air. Because path 7 was closer to the CO source than path 6, the local CO level near path 7 was higher. Moreover, the top portion of the room generally had higher CO levels than the lower, which also contributed to the higher CO concentration near path 7.

Figure 7 only shows one snapshot of the CO distribution at the end of the simulation. In fact, the transient CO distribution in the whole house was determined by many of these snapshots from the CFD calculation. Figure 8 illustrates the time-dependent CO profiles in the utility room, the kitchen and the living room, and the local CO levels near path 6 and 7 by using two methods. One method was when the whole house was simulated by CONTAM (results tagged by “well mixed” in Figure 8) and the other was when the utility room was modeled by CFD0 and the rest of the rooms by CONTAM (results tagged with “CFD” in Figure 8). When the utility room was simulated as a CFD zone, the CO level of the utility room was spatially averaged over the entire room. Figure 8 does not show the results of the bedrooms and the rest of the house, which were much lower than the three rooms shown in the figure. It was shown that CO levels in the utility room fluctuated every 10 minutes with the on/off cycle of the furnace, whether or not CFD was used for the utility room. The simulation using CFD predicted more variable and higher CO concentration in the kitchen than that in the well-mixed case. This difference is due to the high local CO level near airflow path 7 connecting the kitchen and the utility room. Path 7 was very close to the CO source, so variations of CO generation rate could

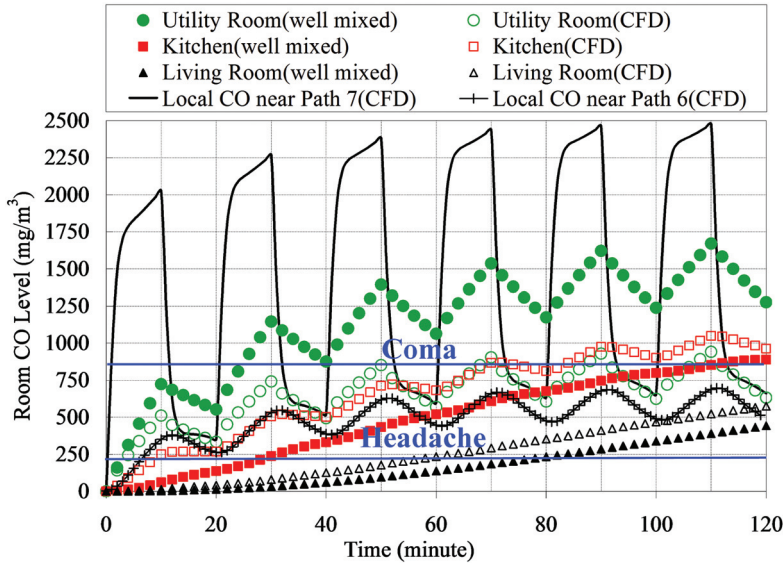


**Figure 8. Comparison of CO levels in utility room, kitchen, and living room of the house with and without CFD simulations.**

easily affect the CO level in the kitchen. Moreover, the peak level of CO near path 7 was significantly higher than that near path 6, which leads to CO concentrations in the utility room to be highly nonuniform. This example illustrates the importance of the source location and the local concentration of CO near interzonal connections.

The CO levels in the non-source zones were similar in magnitude between the CFD and well-mixed case. However, the small difference in CO levels may be important with respect to occupant exposure. The lines in Figure 8 mark two critical CO levels for occupant exposure. The bottom line (“Headache”) corresponds to  $233 \text{ mg/m}^3$  ( $2.3 \times 10^{-4}$  ounce/ft<sup>3</sup>) ( $200 \text{ ppm}_v$ ). Exposure to this level for 1 to 2 hours can cause flu-like symptoms such as headache, lightheadedness, nausea, and fatigue (NIOSH et al. 1996). The upper line (“Coma”) is located at  $815 \text{ mg/m}^3$  ( $8.1 \times 10^{-4}$  ounce/ft<sup>3</sup>) ( $700 \text{ ppm}_v$ ). Exposure to this level for one hour or more can cause more severe CO poisoning, such as progressively worsening symptoms of vomiting, confusion, and coma (NIOSH et al. 1996). The well-mixed simulation (without CFD) is shown to reach either of the two critical lines about 20 minutes later than that with CFD in both the living room and the kitchen. A period of 20 minutes may be crucial in some situations relative to occupant safety and evacuation.

## CONCLUSION

This paper introduced and demonstrated the new CFD features of CONTAM 3.0: the external CFD link for simulations of airflows around a building exterior, and the internal CFD link for embedding a CFD zone within a CONTAM airflow network. The external CFD link predicts distributions of wind pressures and contaminant concentrations outside a building for simulating their effect on indoor contaminant concentrations. The internal CFD zone enables the detailed calculation of air and contaminant concentrations in a room or region of a building for which the well-mixed assumption is insufficient, with the remaining rooms handled with the well-mixed assumption that is typical of CONTAM. These new capabilities were demonstrated by modeling

a generic low-rise residential house. It was shown that the external CFD link generally provides a better estimation of wind pressure profiles and air infiltration than the simulations without CFD. Moreover, the embedded CFD zone is very useful for analysis of short-time contaminant transport, especially for evaluation of occupant exposure. The lack of experimental validations for the specific house studied in this paper limits the ability to fully quantify the improvements in predictive accuracy for the CFD analysis relative to a multizone model. Further experimental studies are definitely needed to obtain such data, which will presumably improve the understanding of these calculation methods. Nevertheless, the new CFD feature of CONTAM 3.0 provides a useful capability for building ventilation design and indoor air quality analysis.

## ACKNOWLEDGMENTS

The authors would like to express their appreciation for the numerous suggestions and comments from George N. Walton and Steven J. Emmerich from the National Institute of Standards and Technology throughout this study, and the invaluable contributions of Brian J. Polidoro, also of NIST, in developing the tools needed to perform this study.

## REFERENCES

- ASHRAE. 2009. Airflow around buildings. Chapter 24 in the 2009 *ASHRAE Handbook—Fundamentals*. Atlanta, GA: ASHRAE.
- ASTM. 2008. Standard guide for statistical evaluation of indoor air quality models. West Conshohocken, PA: American Society for Testing and Materials.
- Bartak, M., I. Beausoleil-Morrison, J.A. Clarke, J. Denev, F. Drkal, M. Lain, I.A. Macdonald, A. Melikov, Z. Popiolek, and P. Stankov. 2002. Integrating CFD and building simulation. *Building and Environment* 37(8-9):865–71.
- Beausoleil-Morrison, I. 2002. The adaptive conflation of computational fluid dynamics with whole-building thermal simulation. *Energy and Buildings* 34(9):857–71.
- Chen, Q., L.R. Glicksman, and J. Srebric. 1999. *Simplified methodology to factor room air movement and the impact on thermal comfort into design of radiative, convective and hybrid heating and cooling systems*. Atlanta, GA: ASHRAE.
- Chen, Q. and W. Xu. 1998. A zero-equation turbulence model for indoor airflow simulation. *Energy and Buildings* 28:137–44.
- Clarke, J.A. 1985. *Energy simulation in building design*. Bristol: Adam Hilger.
- Clarke, J.A., W.M. Dempster, and C.O.R. Negrao. 1995. The implementation of a computational fluid dynamics algorithm within the ESP-r System. *Building Simulation '95 Conference*, Madison, WI. International Building Performance Simulation Association.
- Cochran, L. 2000. Wind engineering as related to tropical cyclones. Chapter 14 in *Storms*, vol. 1. New York: Routledge.
- Gao, Y. 2002. *Coupling of computational fluid dynamics and a multizone airflow analysis program for indoor environmental design*. Cambridge, MA: Massachusetts Institute of Technology.
- Holmes, J.D. 1986. Wind loads on low-rise buildings. Chapter 12 in *The structural and environmental effects of wind on building and structures*. Melbourne: Monash University.
- Holmes, J. D. 1994. Wind pressures on tropical housing. *Journal of Wind Engineering and Industrial Aerodynamics* 53(1–2):105–23.
- Jayaraman, B., D. Lorenzetti, and A. Gadgil. 2004. Coupled model for simulation of indoor airflow and pollutant transport. Berkeley, CA: Lawrence Berkeley National Laboratory.
- Jiang, Y., D. Alexander, H. Jenkins, R. Arthur, and Q. Chen. 2003. Natural ventilation in buildings: measurement in a wind tunnel and numerical simulation with large eddy simulation. *Journal of Wind Engineering and Industrial Aerodynamics* 91(3): 23.
- Lee, S.W. 1990. *Transient emissions associated with various furnace cyclic patterns in residential oil combustion—A laboratory study*. Available from [http://www.anl.gov/PCS/acsfuel/preprint archive/Files/35\\_3\\_WASHINGTON DC\\_08-90\\_0763.pdf](http://www.anl.gov/PCS/acsfuel/preprint archive/Files/35_3_WASHINGTON DC_08-90_0763.pdf).

- Negrao, C.O.R. 1998. Integration of computational fluid dynamics with building thermal and mass flow simulation. *Energy and Buildings* 27(2):155–65.
- NIOSH, CDPHE, CPSC, OSHA, and U.S. EPA. 1996. *ALERT: Preventing carbon monoxide poisoning from small gasoline-powered engines and tool*. National Institute for Occupational Safety and Health, Colorado Department of Public Health and Environment, U.S. Consumer Product Safety Commission, Occupational Safety and Health Administration, and U.S. Environmental Protection Agency. Retrieved December 10, 2009, from <http://www.cdc.gov/niosh/carbon2.html>.
- Persily, A.K. and E.M. Ivy. 2001. *Input data for multizone airflow and IAQ analysis*. Gaithersburg, MD: National Institute of Standard and Technology.
- Ryan, J.V. and R.C. McCrillis. 1994. Analysis of emissions from residential natural gas furnaces. *87th Annual Meeting and Exhibition of the Air & Waste Management Association*, Cincinnati, OH.
- Schaelin, A., V. Dorer, J. van der Maas, et al. 1993. Improvement of multizone model predictions by detailed flow path values from CFD calculations. *ASHRAE Transactions* 99(2):709–20.
- Srebric, J., J. Yuan, and A. Novoselac. 2008. On-site experimental validation of a coupled multizone and CFD model for building contaminant transport simulations. *ASHRAE Transactions* 114(1).
- Srinivas, T. 2001. *Evaluation and enhancement of computational techniques in indoor air quality analysis*. Department of Biological Engineering. Halifax, Nova Scotia, Dalhousie University.
- Swami, M.V. and S. Chandra. 1987. *Procedures for calculating natural ventilation airflow rates in buildings*. Cape Canaveral, Florida Solar Energy Center.
- Swami, M.V. and S. Chandra. 1988. Correlations for pressure distributions on buildings and calculation of natural-ventilation airflow. *ASHRAE Transactions* 94(1):243–66.
- Walton, G.N. 1989. *AIRNET—A computer program for building airflow network modeling*. Gaithersburg, MD, National Institute of Standards and Technology.
- Walton, G.N. and W.S. Dols. 2008. *CONTAMW 2.4 user manual*. Gaithersburg, MD, USA, National Institute of Standards and Technology.
- Wang, L. 2007. *Coupling of multizone and CFD programs for building airflow and contaminant transport simulations*. Ph.D. dissertation. Department of Mechanical Engineering, Purdue University, West Lafayette, IN.
- Wang, L. and Q. Chen. 2007a. Theoretical and numerical studies of coupling multizone and CFD models for building air distribution simulations. *Indoor Air* 17(5):348–61.
- Wang, L. and Q. Chen. 2007b. Validation of a coupled multizone and CFD program for building airflow and contaminant transport simulations. *HVAC&R Research* 13(2):15.
- Wang, L. and Q. Chen. 2008. Evaluation of some assumptions used in multizone airflow network models. *Building and Environment* 43(10):1671–77.
- Wang, L. and S.J. Emmerich. 2010. Modeling the effects of outdoor gasoline powered generator use on indoor carbon monoxide exposures. *Building Simulation* 3(1):39–50.
- Wang, L., S.J. Emmerich, and R. Powell. 2010. *Modeling the effects of outdoor gasoline powered generator use on indoor carbon monoxide exposures—Phase II*. Gaithersburg, National Institute of Standards and Technology: 23.

